Ultraprecise Atomic Mass Measurement of the α Particle and ^{4}He

R. S. Van Dyck, Jr., S. L. Zafonte, S. Van Liew, D. B. Pinegar, and P. B. Schwinberg
Department of Physics, University of Washington, Seattle, Washington 98195-1560, USA
(Received 23 July 2003; published 4 June 2004)

The atomic masses of the α particle and ^{4}He have been measured by means of a Penning trap mass spectrometer which utilizes a frequency-shift detector to observe single-ion cyclotron resonances in an extremely stable 6.0 T magnetic field. The present resolution of this instrument approaches 0.01 ppb [10 ppt (parts per trillion)] and is limited primarily by the effective stability ($<$5 ppt/h) of the magnet over hundreds of hours of observation. The leading systematic shift [at $-202(9)$ ppt] is due to the image charge located in the trap electrodes. The new value for the atomic mass of the α particle is 4 001 506 179.147(64) nu and the corresponding value for the mass of ^{4}He is 4 002 603 254.153(64) nu (nu $= 10^{-9}$ u). The 16 ppt uncertainty is at least 20 times smaller than any previous determination.

DOI: 10.1103/PhysRevLett.92.220802 PACS numbers: 06.20.Jr, 07.75.+h, 32.10.Bi, 82.80.Qx

In the past decade, the single-ion Penning Trap Mass Spectrometer (PTMS) has proven itself to be superior to other instruments capable of determining atomic masses to extremely high precision. This was dramatically illustrated in 1995 by several precise measurements generated by the MIT PTMS [1], obtaining accuracies on the order of 100 parts per trillion (ppt). Then, using our University of Washington (UW) PTMS, we reported in 1998 a measurement of the proton's atomic mass [2] with an accuracy of 140 ppt, for a factor of 4 improvement over that reported in [1]. This was done during the early testing of our rebuilt spectrometer with ions of interest that had mass-to-charge ratios (m/q) differing by a factor of 3. Two years later, we obtained an order of magnitude improvement, illustrated in our new measurement of the atomic mass of ^{16}O with an accuracy of 10 ppt [3]. (Here, the m/q ratios ranged from 2–3u/e for all ions used in this comparison.) The MIT PTMS has the promise of achieving similar accuracies in the future [4] by using two simultaneously trapped ions to mitigate their magnetic field instability problem. The Stockholm PTMS also shows great promise of achieving an improvement that could ultimately approach 100 ppt accuracies [5] in their experiments. The primary motivation of these ultrahigh precision mass spectrometers is to help determine a self-consistent table of atomic masses [6] which can be used in experiments on atomic, nuclear, and particle interactions such as the quest for a microscopic nuclear mass formula [7]. These spectrometers can also be used to determine parameters which may lead to new determinations of some fundamental constants such as the molar Planck constant and the fine-structure constant [8]. For instance, our new determination of the electron's mass [9] contributed to the improved determination of the Rydberg constant [10].

After the ^{16}O measurements were made, the mass of ^{4}He became of interest, partly because a serious discrepancy in its atomic mass was uncovered by the SMILETRAP collaboration [11]. They found a possible 1-ppb difference existed between their recent ^{4}He mass measurements and the old accepted value which had been based on measurements made by the UW PTMS in 1992 (reported in [12]). This measurement was made in an older apparatus, before the magnetic field instability associated with diurnal temperature cycling of the laboratory was known. (The current spectrometer is 2 orders of magnitude less sensitive to this effect.) The mass discrepancy has serious implications because the ^{4}He atomic mass is not only related to the α particle's mass (considered a fundamental constant [13]), but it is often used to establish a chain to link heavier atomic masses to lighter ones in the highly precise least-squares adjustment of all known atomic masses [6]. Our new result will effectively allow ^{4}He to be used as a reference ion for mass comparisons in other spectrometers such as the Stockholm instrument [11].

Our mass spectrometer captures and stores a single ion, and is capable of monitoring all the ion's normal modes of motion. The axial, magnetron, and apparent cyclotron modes have frequencies $\nu_z \approx 3.5$ MHz, $\nu_m \approx 0.14$ MHz, and $\nu_c' \approx 45.4$ MHz, respectively, inside a carefully fabricated five-electrode compensated Penning trap [14]. This device is placed within a custom-designed magnet/cryostat system [15] whose magnetic field ($B = 6$ T) is stabilized by controlling the variations in the pressure of the liquid helium boil-off vapor to $\sim 10^{-3}$ Torr. The ion's mass, $m = qB/2\pi\nu_c$, is derived from the free-space cyclotron frequency, which is obtained from the quadrature sum of all three observed normal mode frequencies:

$$(\nu_c)^2 = (\nu_c')^2 + (\nu_z)^2 + (\nu_m)^2. \quad (1)$$

This equation is valid in spite of any misalignments between the direction of the magnetic field and the trap's electric axis of symmetry [16].

The basic operation of the UW PTMS is described in some detail in the literature [12,17,18]. (An exhaustive theoretical review of single charged particles in Penning

traps is also available [19].) Therefore, the following is a brief outline of the origin of the detected signal, which will help one understand the data we present.

The motion of the single ion is excited along the z axis of symmetry (by a fixed frequency synthesizer) which induces image currents in the end cap electrodes that are in equilibrium with the 4 K environment. One end cap is used to observe this motion by means of an attached parallel LC circuit, tuned to $\nu_z = \sqrt{qV_0/md^2}/(2\pi)$. In this case, the end cap to ring potential difference, V_0, is $\sim$46.6 V and d is the characteristic trap dimension ($\approx$0.211 cm). The resulting signal voltage, which exceeds the thermal noise when observed through our narrow-band detector, is amplified by a cryogenic preamp and mixed with the original phase-shifted drive voltage to generate an error signal. If anything shifts ν_z, the error signal becomes nonzero and is integrated to produce an offset voltage that is fed back to the ring electrode, thus correcting ν_z. In this way, the ion's axial motion is kept frequency locked to the stable drive source, and the effective energy well that the ion mass sees is kept constant. The resulting *correction* voltage (now referred to as the frequency-shift signal) gives real-time information about perturbations to the ion's axial motion.

We detune the voltage on the trap compensation electrodes to produce a small anharmonic term ($\propto r^4$) [17] so that the correction voltage now depends slightly on the radial position of the trapped ion. Figure 1 shows the frequency-shift signal for a C^{6+} ion when an appropriate rf-drive field has its frequency swept through the *undamped* cyclotron resonance in both directions. Of particular note is the asymmetry associated with sweep direction [20]. The correction voltage in the down sweep reaches a corner and becomes a sloped straight line, with ν_c' continuously shifted just slightly down frequency by the relativistic mass increase as the orbit becomes larger. For the up sweep response, ν_c' is pulled *through* the drive frequency as energy is absorbed. In this case, the frequency-shift signal appears as a step function, filtered through the detector time constant. Consecutive up sweep and down sweep serve to bracket the resonance and generate observations of ν_c' versus time. However, this asymmetric process causes a systematic error which requires our attention (see below).

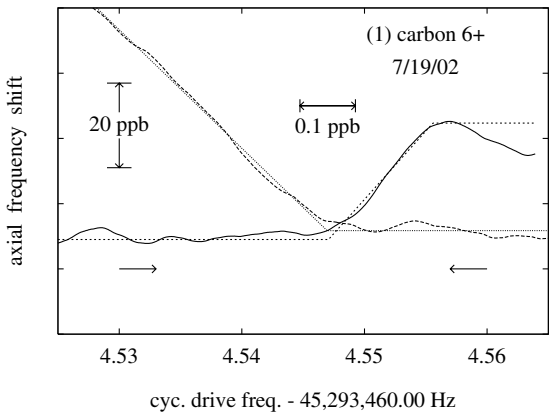

FIG. 1. The bracketed cyclotron resonance for a single C^{6+} ion using our anharmonic detection method. The superimposed straight line segments are least-squares fitted lines and the typical relative "linewidth" (between corner frequencies) is 100–200 ppt. In comparison, the actual physical linewidth is $\sim$30 ppb, dominated by fluctuations in battery potential.

Our Penning trap contains additional electrodes (located within each end cap) that fold an electron beam from a field-emission point (FEP) back on itself, in order to optimize the probability of generating a fully stripped carbon ion in about a minute from $\sim$10 nA of electrons released from the FEP. Both carbon and helium are obtained from gases absorbed onto metal surfaces which are either scrubbed by the electron beam or released by resistive heating of a source. Because various charge states of all background gases are produced in this process, the crucial next step requires great care to throw out unwanted ions. This cleaning is accomplished by the use of suitably strong noise-broadened rf drives at the axial frequencies of the unwanted ions. The remaining cloud of ions of interest is reduced to a single by lowering the potential on the trap until the effective well depth is $<$0.1% of its normal value.

Next, the ion's magnetron and cyclotron orbits are systematically minimized by the application of rf drives at $\nu_z + \nu_m$ [21] and $\nu_c' - \nu_z$ [22], respectively, in order to prepare a reproducible initial state before each excitation of the cyclotron motion. Then, ν_c' is measured for each ion using the frequency-shift detector. These data can be displayed on the same plot when scaled by the appropriate cyclotron frequency ratio [CFR $\equiv \nu_c(He^{2+})/\nu_c(C^{6+})$]. As an example, the data shown in Fig. 2 compares 85 h of helium 2+ data versus 67 h of carbon 6+ data, with a relative statistical error of about 25 ppt.

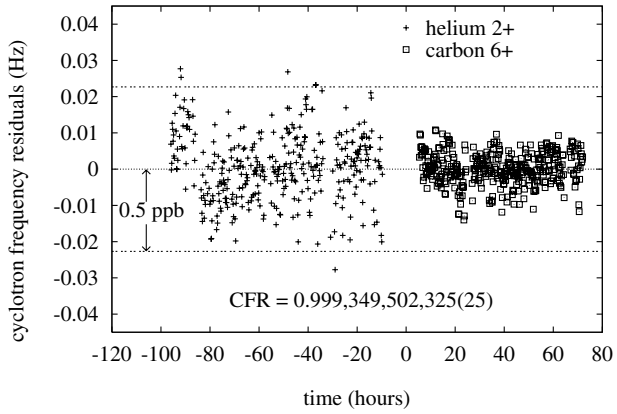

FIG. 2. Plot of cyclotron frequency residuals versus time for 60% of run No. 6. A small linear drift (3.3 ppt/h) has been removed from the resonance frequencies and the C^{6+} data have been scaled by the cyclotron frequency ratio (as shown).

The most critical part of any extremely high precision measurement is the analysis of possible systematics. For our spectrometer, this involves noting any shift in the observed cyclotron frequency when we vary the rf power associated with the drives used in the initial preparation for a sweep, or those drives that later excite the axial and cyclotron motions. In some cases, it was determined that even a 6–10 dB increase in power produced no noticeable shift (i.e., well below the statistical error of the data involved). Such is the case for the dependence on cyclotron drive power which is statistically consistent with zero (also shown in [3]). However, we did identify three directly measurable effects (at the current level of precision), as described below.

The first is an image-charge shift associated with an ion inside a finite metallic cavity. This shift depends only on the amount of charge in the center of mass, and not on the specific ion species itself [23]. It has recently been investigated for the present trap by measuring ν_c' versus the number of trapped ions for both O^{6+} and C^{6+}, yielding a frequency correction of $+2.3(1)$ mHz/trapped charge [3]. This applies a shift to the CFR of $-202(9)$ ppt.

The second is a type of "light shift" that is associated with the axial drive field being applied during the excitation of the cyclotron motion [2]. It arises from a weak coupling of the radial normal modes to the axial motion via small perturbations in the uniform magnetic field and in the *slightly* anharmonic electric trapping field. (See Ref. [24] for detailed treatment of nonquadratic terms in the trapping potential.) This shift is determined for *each* trapped ion (for every run) by measuring ν_c' versus axial drive and then extrapolating linearly to zero power.

The last of these directly measurable shifts is associated with the asymmetry in the method of bracketing the cyclotron resonance via consecutive up and down sweeps. We recently investigated this effect by measuring ν_c' with double and triple the sweep range (using the same total sweep time). The observed effect on either ion is a negative shift in ν_c' on the order of 30–60 ppt, for sweeps on the order of 50–100 mHz. This may seem large, but to first order the effect cancels if we use the same sweep range for the ion of interest and the calibration ion (assuming they have roughly the same ν_c'). In the current measurements, we are required to correct for the difference in ranges in all runs except the last one.

There is an additional *indirectly* determined systematic effect due to the locking phase of the axial drive. Quite simply, if the phase set on our detector is incorrect, the error signal does not have a true dispersion line shape; thus, the axial resonance becomes locked to a point displaced from the natural frequency ν_z, which appears in Eq. (1). To avoid this, we sweep out the axial response versus drive frequency and then fit this resonance to a theoretical line shape. The phase is then adjusted until the fitted offset phase error is zero, within some measurable limits. Finally, the effect of this uncertainty on a cyclotron resonance frequency is computed [3] and added in quadrature with the other appropriate measurement uncertainties. Our model was recently checked by carefully measuring ν_c' versus axial phase for C^{6+} over a range of $\pm 30°$. The measured results were found to agree within 10% of our prediction, consistent within the uncertainty of the measured axial linewidth (one of the line shape fitting parameters).

Table I summarizes the eight $^4He^{2+}/^{12}C^{6+}$ runs taken in our present spectrometer with the corresponding uncertainties of the effects previously described. We have estimated the CFR and its error for each run to cover the distribution of multiple trial fits to the available data. Different trials correspond to parsing the data 3 or 4 times as if the run had been taken over consecutively smaller periods of time, centered on the transition to the calibration ion. For each parsing of the data, the basic time variation is assumed to be either strictly linear or containing a small quadratic dependence. In addition, some of the trials include a correction for the wander in ambient temperature or ambient pressure. Figure 2 is an example trial fit to 60% of run No. 6 with a linear drift removed, but no corrections made for variations in ambient temperature or pressure.

The value chosen for the statistical uncertainty is roughly double the fit error (i.e., the one that yields a unity reduced chi squared) found for the fit trial which uses all the data available in a given run. In all cases, the chosen uncertainty is larger than the fit error of any single fit trial. Since the overall chi squared for all eight runs is 0.41, it is clear that we have conservatively overestimated the statistical error. We justify this choice because of our concern that background contaminant ions may cause a wander in ν_c' with time due to variations in the center-of-mass motion. After completing the first seven runs in this sequence, we became much more concerned about this possibility. In run No. 8, we took still greater care to minimize any possible contamination, and to reduce the other systematics. The magnitude of the applied shifts, the subsequent errors associated with each effect, and the magnitude of the statistical uncertainty demonstrate this additional effort.

The weighted average obtained from the last column in Table I yields the final CFR $\mathrm{CFR} = 0.999\,349\,502\,354\,8(13\,4)$ where the 13.4 ppt uncertainty represents the error that could conceivably be reduced with further measurements, either within each run or with more runs. This result includes the *shift* due to the image-charge effect, but not its *uncertainty* since this systematic is common to all runs and is independently measured. To convert the CFR (now with all uncertainties included) to the α particle's atomic mass, the masses of the electrons removed from ^{12}C, plus the relativistic mass from their binding energies [25], are restored to yield

$$M_\alpha = 4\,001\,506\,179.147(64)\ \mathrm{nu}$$

TABLE I. Summary of $^4He^{2+}/12C^{6+}$ comparisons with relative systematic shifts. All shifts are in ppt (10^{-12}) of CFR. In the last column, $\Delta(\mathrm{CFR}) \equiv (\mathrm{CFR} - 0.999\,349\,502\,000) \times 10^{12}$.

Run No.	Run's start date	Days in run	Statistical error	Axial drive shift	Axial drive error	Phase shift	Phase error	Range-fit shift	Range-fit error	Δ(CFR)
1	11/07/00	12	33.0	−106	7.9	−17.0	25.7	+26.0	2.6	359.6(42.6)
2	12/06/00	11	48.7	−133	17.3	0	24.0	+24.0	2.4	369.2(57.0)
3	12/23/00	17	38.0	−175	29.2	0	12.8	+32.5	3.3	347.5(49.7)
4	01/19/01	15	51.0	−106	10.4	0	14.6	+26.0	2.6	430.5(54.1)
5	08/22/01	18	39.0	−135	6.4	0	13.3	−6.5	0.7	357.7(41.7)
6	10/14/01	10	32.0	−36.4	4.9	0	12.6	+26.0	2.6	325.1(34.8)
7	11/19/01	11	40.0	−37.7	7.0	0	12.9	+54.6	5.5	340.3(43.0)
8	08/16/02	8	14.0	−126	10.6	0	14.4	0	0	355.1(22.7)

(where nu $= 10^{-9}$ u). Finally, making similar corrections for lost electron masses and binding energies for helium, we determine a new value for the atomic mass for ^{4}He,

$$M(^4\mathrm{He}) = 4\ 002\,603\,254.153(64)\ \mathrm{nu}.$$

This result can be compared to the most recently reported values obtained by the University of Mainz researchers [26], $M(^4\mathrm{He}) = 4\,002\,603\,248.9(2.2)$ nu, and the University of Stockholm SMILETRAP collaboration [27], $M(^4\mathrm{He}) = 4\,002\,603\,256.8(1.3)$ nu. Our result is consistent with these other measurements at the 2σ level, but is ~20 times more accurate.

This manuscript is based upon work supported by the National Science Foundation under Grant No. 0097277.

[1] F. DiFilippo, V. Natarajan, M. Bradley, F. Palmer, and D. E. Pritchard, Phys. Scr. **T59**, 144 (1995).
[2] R. S. Van Dyck, Jr., D. L. Farnham, S. L. Zafonte, and P. B. Schwinberg, in *Trapped Charged Particles and Fundamental Physics*, AIP Conf. Proc. No. 457 (AIP, New York, 1999), pp. 101–110.
[3] R. S. Van Dyck, Jr., S. L. Zafonte, and P. B. Schwinberg, Hyperfine Interact. **132**, 163 (2001).
[4] S. Rainville, J. K. Thompson, and D. E. Pritchard, *Conference on Precision Electromagnetic Measurements* (IEEE, Piscataway, NJ, 2002), Catalog No. 02CH37279, pp. 318; see also Science **303**, 334 (2004).
[5] T. Fritioff, H. Bluhme, R. Schuch, I. Bergstrom, and M. Bjorkhage, Eur. Phys. J. A **15**, 249 (2002).
[6] G. Audi and A. H. Wapstra, Nucl. Phys. **A565**, 1 (1993); **A595**, 409 (1995); also at http://csnwww.in2p3.fr/amdc/.
[7] J. M. Pearson, Hyperfine Interact. **132**, 59 (2001).
[8] M. P. Bradley, J. V. Porto, S. Rainville, J. K. Thompson, and D. E. Pritchard, Phys. Rev. Lett. **83**, 4510 (1999).
[9] D. L. Farnham, R. S. Van Dyck, Jr., and P. B. Schwinberg, Phys. Rev. Lett. **75**, 3598 (1995).
[10] C. Schwob *et al.*, Phys. Rev. Lett. **82**, 4960 (1999).
[11] T. Fritioff, C. Carlberg, G. Douysset, R. Schuch, and I. Bergstrom, Hyperfine Interact. **132**, 231 (2001); I. Bergstrom (private communication).
[12] R. S. Van Dyck, Jr., D. L. Farnham, and P. B. Schwinberg, Phys. Scr. **T59**, 134 (1995).
[13] P. J. Mohr and B. N. Taylor, Rev. Mod. Phys. **72**, 351 (2000).
[14] R. S. Van Dyck, Jr., D. J. Wineland, P. A. Ekstrom, and H. G. Dehmelt, Appl. Phys. Lett. **28**, 446 (1976).
[15] R. S. Van Dyck, Jr., D. L. Farnham, S. L. Zafonte, and P. B. Schwinberg, Rev. Sci. Instrum. **70**, 1665 (1999).
[16] L. S. Brown and G. Gabrielse, Phys. Rev. A **25**, 2423 (1982).
[17] F. L. Moore *et al.*, Phys. Rev. A **46**, 2653 (1992).
[18] R. S. Van Dyck, Jr., in *Atomic. Molecular, and Optical Physics: Charged Particles*, edited by R. Hulet and B. Dunning (Academic, New York, 1995), Vol. 29A, pp. 363–389.
[19] L. S. Brown and G. Gabrielse, Rev. Mod. Phys. **58**, 233 (1986).
[20] T. P. Heavner, S. R. Jefferts, and G. H. Dunn, Phys. Rev. A **64**, 62504 (2001).
[21] R. S. Van Dyck, Jr., P. B. Schwinberg, and H. G. Dehmelt, in *New Frontiers in High Energy Physics*, edited by B. Kursunoglu, A. Perlmutter, and L. F. Scott (Plenum, New York, 1978), pp. 159–181.
[22] R. S. Van Dyck, Jr., D. L. Farnham, and P. B. Schwinberg, J. Mod. Opt. **39**, 243 (1992).
[23] R. S. Van Dyck, Jr., F. L. Moore, D. L. Farnham, and P. B. Schwinberg, Phys. Rev. A **40**, 6308 (1989).
[24] G. Gabrielse, Phys. Rev. A **27**, 2277 (1983).
[25] R. L. Kelly, J. Phys. Chem. Ref. Data **16**, 1 (1987).
[26] S. Brunner, T. Engel, H. Klein, A. Schmitt, and G. Werth, Eur. Phys. J. D **15**, 181 (2001).
[27] T. Fritioff, C. Carlberg, G. Douysset, F. Schuch, and I. Bergstrom, Eur. Phys. J. D **15**, 141 (2001).